Electronic Journal of Differential Equations, Vol. 2024 (2024), No. 08, pp. 1–19.
ISSN: 1072-6691. URL: https://ejde.math.txstate.edu, https://ejde.math.unt.edu
DOI: 10.58997/ejde.2024.08

OPTIMAL MASS OF STRUCTURE WITH MOTION DESCRIBED BY STURM-LIOUVILLE OPERATOR: DESIGN AND PREDESIGN

BORIS P. BELINSKIY, TANNER A. SMITH

Abstract. We find an optimal design of a structure described by a Sturm-Liouville (S-L) problem with a spectral parameter in the boundary conditions. Using an approach from calculus of variations, we determine a set of critical points of a corresponding mass functional. However, these critical points - which we call predesigns - do not necessarily themselves represent meaningful solutions: it is of course natural to expect a mass to be real and positive. This represents a generalization of previous work on the topic in several ways. First, previous work considered only boundary conditions and S-L coefficients under certain simplifying assumptions. Principally, we do not assume that one of the coefficients vanishes as in the previous work. Finally, we introduce a set of solvability conditions on the S-L problem data, confirming that the corresponding critical points represent meaningful solutions we refer to as designs. Additionally, we present a natural schematic for testing these conditions, as well as suggesting a code and several numerical examples.

1. Introduction

This paper represents a continuation of the work done in [7]. Historically, the first study in this direction was performed by Turner [20], who used techniques from the calculus of variations to determine an optimal cross-sectional mass distribution for a rod of a given principal eigenfrequency ω with the least possible mass. The construction he found allows for greater economy in a design that meets a requirement for this given natural frequency. The longitudinal oscillations $u(x,t)$ of the rod are modeled by the wave equation

$$mu_{tt} = \frac{E}{\rho}(mu_x)_x = 0,\ 0 < x < L. \tag{1.1}$$

Here E is Young's modulus, ρ is density of the material, and $m(x)$ is mass per unit length. The rod is considered fixed at the left end and attached to a mass M_1 at the right end. After separating variables and removing the harmonic term $e^{i\omega t}$, the following optimization problem appears.

2020 *Mathematics Subject Classification.* 34L15, 74P05, 49K15, 49S05, 49R05.
Key words and phrases. Sturm-Liouville problem; vibrating rod; calculus of variations; optimal design; boundary conditions with spectral parameter.

Submitted August 6, 2023. Published January 24, 2024.

Problem 1.1. Consider the Sturm-Liouville (S-L) problem

$$E(mu_x)_x + \omega^2 \rho u = 0,\ 0 < x < L, \tag{1.2}$$

$$u(0) = 0, \quad E(mu_x)(L) = \omega^2 \rho M_1 u(L). \tag{1.3}$$

Find the mass distribution $m(x)$ such that the total mass functional

$$M[m] := \int_0^L m(x)dx$$

attains its minimum value.

Note that the boundary condition contains the spectral parameter ω^2 linearly. It is easy to show that the spectral parameter $\omega^2 > 0$. Indeed,

$$\omega^2 = \frac{\int_0^L Emu_x^2\,dx}{\int_0^L \rho u^2\,dx + \rho M_1 u^2(L)}\,. \tag{1.4}$$

To solve this optimization problem, Turner reformulates it to optimize the functional

$$\begin{aligned} F[m,u] := M[m] + \int_0^L \Lambda(x)[E(mu_x)_x + \omega^2 \rho u]\,dx \\ + \lambda_1[E(mu_x)(L) - \omega^2 \rho M_1 u(L)], \end{aligned} \tag{1.5}$$

where Λ and λ_1 are Lagrange multipliers. Using the techniques of calculus of variations [11] Turner found the optimal mass distribution

$$m_{\rm opt}(x) = m(L)\cosh^2(\gamma L)/\cosh^2(\gamma x) \tag{1.6}$$

where

$$m(L) = M_1 \tanh \gamma L,\ \gamma := \omega^2 \rho / E.$$

Of course, Turner's technique may also be, in a sense, reversed to determine the optimal cross-sectional mass distribution such that a rod of a given total mass is made with the largest principle eigenfrequency. The applications of such techniques are complementary: a mass can be optimized to meet a certain given natural frequency, or a rod of a given mass may be optimized to yield the greatest resistance to resonance. Taylor [19] considered this problem and articulated the duality of these complementary optimization problems employed in [20] in a form that assists in generalizing the method.

The next step was made in [7], where the authors considered the linear second-order S-L problem

$$(py')' - qy + \lambda_1 pry = 0, \quad x \in (0,1), \tag{1.7}$$

$$\cos(\alpha)y(0) + \sin(\alpha)p(0)y'(0) = 0, \tag{1.8}$$

$$-\beta_1 y(1) + \beta_2 p(1)y'(1) = \lambda_1[\beta_1' y(1) - \beta_2' p(1)y'(1)]. \tag{1.9}$$

The original problem (1.2)-(1.3) appears if we let

$$p(x) = Em(x), \quad q \equiv 0, \quad r(x) = \frac{\rho}{Em(x)}, \quad \lambda = \omega^2\,.$$

A significant generalization in [7] is made in the boundary conditions as compared to [19] and [20], but it is assumed that $q \equiv 0$.

For the general theory on problem (1.7)-(1.9) with arbitrary q see [1, 22]. Our notations are adopted from [3, 9, 10, 12, 17, 21]. Additionally, we follow the restrictions on the coefficients p, q, r, as outlined in these works, to guarantee our

S-L problem is self-adjoint - and thus that all eigenvalues are real. To that end, we proceed under the following assumptions on the functions p, r, q and constants α, β_j, β_j' ($j = 1, 2$).

Assumptions. We use the following assumptions on the parameters of our S-L problem

(1) $p \in C^1[0,1]$, $q, r \in C[0,1]$;
(2) $p, r > 0$ for all $x \in [0,1]$;
(3) The parameters $\beta_j, \beta_j' \in \mathbb{R}$ satisfy $\delta := \beta_1'\beta_2 - \beta_1\beta_2' > 0$;
(4) $\alpha \in [0, \pi)$.

We will refer to the set $\{\alpha, \beta_1, \beta_2, \beta_1', \beta_2', \lambda_1, q, r\}$ as our *data set* $\mathscr{D}$. The mass functional to be minimized is

$$M[p] := \int_0^1 pr dx. \tag{1.10}$$

The authors of [7] formulated an isoperimetric problem in terms of a functional similar to (1.5),

$$\begin{aligned} F[y,p] := M[p] &+ \int_0^1 \Lambda_1(x)[((py')' + \lambda_1 pry)]\,dx \\ &+ \Lambda_2[\cos(\alpha)y(0) + \sin(\alpha)p(0)y'(0)] \\ &+ \Lambda_3([-\beta_1 y(1) + \beta_2 p(1)y'(1)] - \lambda_1[\beta_1' y(1) - \beta_2' p(1)y'(1)]) \end{aligned} \tag{1.11}$$

with Lagrange multipliers $\Lambda_1(x)$, Λ_2, Λ_3. This functional accumulates the *mass* functional (1.10) - the object to be minimized - with the constraints given by the S-L problem (1.7)-(1.9). Using the methods of the calculus of variations, the authors of [7] derived the expressions for two critical points of the functional $F[y,p]$ in terms of the elementary functions. They also studied a similar optimization problem for a complete bipartite graph (a star).

There are a few mechanical models described by the S-L problem with the spectral parameter in the boundary conditions. Among those are oscillations of a rotating string, a Timoshenko–Mindlin beam with a tip mass, and a rotating beam with a tip mass that models a propeller (see, e.g., [4, 2]). The current study was also motivated by the work of [13] where the authors consider oscillations of a string fixed at one end with a mass connected to a spring at the other end and minimize the first eigenvalue subject to a fixed total mass constraint. The inverse problem for the S-L operator with a spectral parameter in the boundary conditions is actively studied for different models (see, e.g., [16, 14]).

Our work is a continuation of [7] - and thereby [20, 19] - that adds upon the earlier work by the inclusion of several factors. First, the authors of [7] claim that "the calculations of the optimal form for $q \not\equiv 0$ seem to be intractable in the frame of an analytic approach" and hypothesize that "the complete analysis here is possible only at the numerical level," e.g., based on the discretization as in [5, 6, 8]. We instead have found analytical solutions with no such restrictions on q. In fact, we find additional designs dependent on $q \not\equiv 0$. Second, earlier work did not necessarily guarantee the positivity of the function p (and thus the self-adjointness of the S-L operator). To address this issue we introduce the following definition.

Definition 1.2. For a given critical pair (y, p) with a given data set $\mathscr{D}$,

(1) Our solvability conditions are the set of conditions on $\mathscr{D}$ that ensure $p > 0$ on the entire domain.
(2) A predesign is a critical point with no consideration given to solvability conditions.
(3) Once a critical pair has passed our solvability conditions, we refer to it as a design.

In short, we refer to critical points of our isoperimetric problem as *predesigns* while we refer to physically reasonable solutions as *designs*. With these additions in mind, we arrive at the following problem.

Problem 1.3. Consider the S-L problem as described in (1.7)-(1.9) allowing for nonzero q. Find the critical points - potential minimizers - of the mass functional (1.10).

Remark 1.4. For what follows, the sign of the eigenvalue λ_1 is important. Some of these eigenvalues may be negative. It is known that for the S-L problem (1.7)-(1.9), the number of negative eigenvalues is at most finite. In the main part of the text, we assume that $\lambda_1 > 0$ and make a short remark at the end on the results for $\lambda_1 \leq 0$.

After the use of the methods of the calculus of variations to find critical points of the "mass" functional, i.e., functions $p(x)$ and $y(x)$, we find the following critical points as potential minimizers.

Theorem 1.5. *For a given data set $\mathscr{D}$, the mass functional* (1.11) *has critical points*

$$
\begin{gathered}
y_1(x) = \frac{1}{\sqrt{\lambda_1}} \sinh(\sqrt{\lambda_1} g(x) + C_1), \\
p_1(x) = \frac{\int_0^x q(s)\sinh(2\sqrt{\lambda_1}g(s) + 2C_1)ds}{2\sqrt{\lambda_1 r(x)}\cosh^2(\sqrt{\lambda_1}g(x) + C_1)} + C_3 \frac{\sqrt{r(0)}\cosh^2(C_1)}{\sqrt{r(x)}\cosh^2(\sqrt{\lambda_1}g(x) + C_1)}, \\
y_2(x) = \frac{1}{\sqrt{\lambda_1}} \cosh(\sqrt{\lambda_1} g(x) + C_2), \\
p_2(x) = \frac{\int_0^x q(s)\sinh(2\sqrt{\lambda_1}g(s) + 2C_2)ds}{2\sqrt{\lambda_1 r(x)}\sinh^2(\sqrt{\lambda_1}g(x) + C_2)} + C_4 \frac{\sqrt{r(0)}\sinh^2(C_2)}{\sqrt{r(x)}\sinh^2(\sqrt{\lambda_1}g(x) + C_2)}.
\end{gathered}
$$

where the constants C_j are uniquely determined by (1.8) *and* (1.9)*; and we define*

$$
g(x) := \int_0^x \sqrt{r(s)}ds.
$$

We devote subsection 2.1 to the proof of this theorem while the derivation of the constants C_j is found in subsection 2.2. It is also natural to expect that even though we have an analytical form for p, our criterion $p > 0$ for all x will only be met for certain data set $\mathscr{D}$ as we will show in subsection 2.3.

Definition 1.6. We introduce the complementary sets of functions

$$
\begin{gathered}
\mathscr{P} := \{p \in C^1[0,1] : p(x) > 0 \,\forall x \in [0,1]\}, \\
\mathscr{P}^c := \{p \in C^1[0,1] : p(x) \ngtr 0 \,\forall x \in [0,1]\}.
\end{gathered}
$$

That is to say, sets of p that do and do not meet our criteria for solvability.

Remark 1.7. The preceding two sets of functions are nonempty. Further, we will show that we may construct data sets $\mathscr{D}_1$ and $\mathscr{D}_2$ which contain arbitrarily close elements - yet generate $p_1 \in \mathscr{P}$ and $p_2 \in \mathscr{P}^c$, respectively.

Actually, [20] and then [7] substitute the classical statement of the problem based on the solution of the S-L by a variational problem. The last may produce $p \not> 0$, which contradicts the original assumption on p for the regularity of the S-L problem - the singular case is beyond the scope of this work. It may even be in this case that $M[p] \not> 0$, which makes no physical sense in the model used by [20]. Hence, the set $\mathscr{P}^c$ is only of interest in as much as it must be understood to be avoided. To that end, we devote subsection 2.3 to a description of the conditions on $\mathscr{D}$ so that a function p may indeed be a design - and therefore belongs to $\mathscr{P}$. Once we have constructed our critical points and attendant solvability conditions, we explore some numerical examples and special cases in Section 3. This includes an exploration of Remark 1.7.

2. Critical points and solvability conditions of problem 1.1: proof of Theorem 1.5

To construct our solutions, we use the path set out by [7]. However, we include the added term qy which introduces additional complications not previously discussed as well as formulate our solvability conditions. Note that we skip some simple but cumbersome calculations; for all details, see [18].

2.1. Proof of Theorem 1.5.

We formulate an isoperimetric problem in terms of the following functional that represents a generalization of (1.5), (1.11).

$$\begin{aligned} F[y,p] := M[p] &+ \int_0^1 \Lambda_1((py')' - qy + \lambda_1 pry)dx + \Lambda_2(\cos(\alpha)y(0) \\ &+ \sin(\alpha)p(0)y'(0)) + \Lambda_3([-\beta_1 y(1) + \beta_2 p(1)y'(1)] \\ &- \lambda_1[\beta_1' y(1) - \beta_2' p(1)y'(1)]) \end{aligned} \tag{2.1}$$

with Lagrange multipliers $\Lambda_1(x), \Lambda_2, \Lambda_3$. We compute the first variation, δF, of our functional

$$\begin{aligned} \delta F = &\int_0^1 \delta p(r + \Lambda_1\lambda_1 ry - \Lambda_1' y')dx + \int_0^1 \delta y(-\Lambda_1 q + \Lambda_1\lambda_1 rp + (\Lambda_1' p)')dx \\ &+ (\Lambda_1 y'\delta p)|_0^1 + (\Lambda_1 p\delta y')|_0^1 - (\Lambda_1' p\delta y)\big|_0^1 + \Lambda_2(\cos(\alpha)\delta y(0) \\ &+ \sin(\alpha)(y'(0)\delta p(0) + p(0)\delta y'(0))) \\ &+ \Lambda_3([-\beta_1\delta y(1) + \beta_2(y'(0)\delta p(1) + p(1)\delta y'(1))] \\ &- \lambda_1[\beta_1'\delta y(1) - \beta_2'(y'(1)\delta p(1) + p(1)\delta y'(1))]). \end{aligned} \tag{2.2}$$

Here we employ the fundamental lemma of the calculus of variations which guarantees that if $\delta F = 0$ then

$$\delta p: \quad r + \Lambda_1\lambda_1 ry - \Lambda_1' y' = 0, \tag{2.3}$$

$$\delta y: \quad \Lambda_1 q - \Lambda_1\lambda_1 rp - (\Lambda_1' p)' = 0. \tag{2.4}$$

If we isolate incidents of independent variations $\delta y(l)$, $\delta y'(l)$, and $\delta p(l)$ ($l \in \{0,1\}$) in (2.2) we find that

$$\begin{cases} \delta y(0): & \Lambda_2 \cos\alpha - \Lambda_1'(0)p(0) = 0, \\ \delta y'(0): & p(0)(\Lambda_2 \sin\alpha + \Lambda_1(0)) = 0, \\ \delta p(0): & y'(0)(\Lambda_2 \sin\alpha + \Lambda_1(0)) = 0. \end{cases} \tag{2.5}$$

$$\begin{cases} \delta y(1): & \Lambda_1' p(1) - \Lambda_3(\beta_1 + \lambda_1 \beta_1') = 0, \\ \delta y'(1): & \Lambda_1 p(1) - \Lambda_3 p(1)(\beta_2 + \lambda_1 \beta_2') = 0, \\ \delta p(1): & \Lambda_1(1) y'(1) - \Lambda_3 y'(1)(\beta_2 + \lambda_1 \beta_2') = 0. \end{cases} \tag{2.6}$$

From (2.5) we derive

$$\Lambda_1'(0)p(0)/\cos\alpha = \Lambda_2 = -\Lambda_1(0)/\sin\alpha.$$

Similarly from (2.6) we have

$$\Lambda_1'(1)p(1)/(\beta_1 + \lambda_1\beta_1') = \Lambda_3 = \Lambda_1(1)/(\beta_2 + \lambda_1\beta_2').$$

Thus we have conditions independent of Λ_2 and Λ_3,

$$\Lambda_1'(0)p(0)\sin\alpha + \Lambda_1(0)\cos\alpha = 0, \tag{2.7}$$

$$-\Lambda_1'(1)p(1)\beta_2 + \Lambda_1(1)\beta_1 = \lambda_1[\beta_2'\Lambda_1'(1)p(1) - \Lambda_1(1)\beta_1']. \tag{2.8}$$

Note that the boundary value problem from (2.4), (2.7), and (2.8) matches the boundary value problem from (1.7)-(1.9). The eigenspace for this type of problem is well-known to be 1-dimensional with a principal eigenvalue of multiplicity 1. Hence, $\Lambda_1 = \pm\kappa y$ where κ is some arbitrary nontrivial positive constant - we in fact assume without loss of generality that $\kappa = 1$. We see that if we use $\Lambda_1 = y$ in (2.4), (2.7), (2.8), y satisfies the original S-L problem (1.7)-(1.9). If we make a similar substitution into (2.3), we have

$$(y')^2 - \lambda_1 r y^2 = r. \tag{2.9}$$

This nonhomogeneous first-order ODE has two solutions

$$y_1(x) = \frac{1}{\sqrt{\lambda_1}} \sinh(\sqrt{\lambda_1} g(x) + C_1), \tag{2.10}$$

$$y_2(x) = \frac{1}{\sqrt{\lambda_1}} \cosh(\sqrt{\lambda_1} g(x) + C_2), \tag{2.11}$$

where g is as defined in theorem 1.5 and C_j, $j = 1,2$ are arbitrary constants. With the known y_k, $k = 1,2$ we return to the S-L problem with boundary conditions given by (1.8)-(1.9) to solve for corresponding p_k. Upon rearranging (1.7) accordingly, we find that in the situation with unknown p and all other known parameters, we have first-order nonhomogeneous ODE given by

$$p'(x) + \frac{y''(x) + \lambda_1 r(x) y(x)}{y'(x)} p(x) = q(x)\frac{y(x)}{y'(x)}. \tag{2.12}$$

We find using y_1 and y_2, respectively, the solutions to (2.12),

$$p_1(x) = \frac{\int_0^x q(s)\sinh(2\sqrt{\lambda_1}g(s) + 2C_1)ds}{2\sqrt{\lambda_1 r(x)}\cosh^2(\sqrt{\lambda_1}g(x) + C_1)} + C_3\frac{\sqrt{r(0)}\cosh^2(C_1)}{\sqrt{r(x)}\cosh^2(\sqrt{\lambda_1}g(x) + C_1)}, \tag{2.13}$$

$$p_2(x) = \frac{\int_0^x q(s)\sinh(2\sqrt{\lambda_1}g(s) + 2C_2)ds}{2\sqrt{\lambda_1 r(x)}\sinh^2(\sqrt{\lambda_1}g(x) + C_2)} + C_4\frac{\sqrt{r(0)}\sinh^2(C_2)}{\sqrt{r(x)}\sinh^2(\sqrt{\lambda_1}g(x) + C_2)}. \tag{2.14}$$

Here C_j, $j = 1, 2, 3, 4$ are constants determined by (1.8) and (1.9). Thus we have determined the pairs (y_1, p_1) and (y_2, p_2) which represent the critical points of our functional (2.1) - concluding our proof of Theorem 1.5. □

Remark 2.1. (a) We note that if $q(x) \equiv 0$, we recover the critical points from [7]. (b) Finding the constants C_j appears to be quite a nontrivial procedure. We devote the following subsection to their calculation.

2.2. **Determining constants C_j in Theorem 1.5.** The following objects appear naturally in our determination of constants C_j, and we find it useful to highlight them especially.

$$\phi := -\frac{p(0)y'(0)}{y(0)} = \cot\alpha, \tag{2.15}$$

$$\psi := \frac{p(1)y'(1)}{y(1)} = \frac{\beta_1 + \lambda_1\beta_1'}{\beta_2 + \lambda_1\beta_2'}, \tag{2.16}$$

$$\zeta := -\frac{\phi + \psi\cosh(2\sqrt{\lambda_1}g(1)) - \int_0^1 q(s)\cosh(2\sqrt{\lambda_1}g(s))ds}{\psi\sinh(2\sqrt{\lambda_1}g(1)) - \int_0^1 q(s)\sinh(2\sqrt{\lambda_1}g(s))ds}, \tag{2.17}$$

$$z =: \frac{1}{2}\coth^{-1}(\zeta). \tag{2.18}$$

Further, we use the boundary condition (1.8) of our problem to create three cases for each critical function p, for a total of six cases explained in Table 1 below.

Table 1. Summary of predesigns by case

Case	$y_j(x), p_j(x)$	α	Predesign	$M[p_j]$
1	$y_1(x), p_1(x)$	$\alpha = 0$	(2.19)	(2.33)
2	$y_1(x), p_1(x)$	$\alpha = \pi/2$	(2.20)	(2.34)
3	$y_1(x), p_1(x)$	$\alpha \in (0,\pi)\backslash\{\pi/2\}$	(2.25)	(2.35)
4	$y_2(x), p_2(x)$	$\alpha = 0$	(2.19)	(2.33)
5	$y_2(x), p_2(x)$	$\alpha = \pi/2$	(2.20)	(2.34)
6	$y_2(x), p_2(x)$	$\alpha \in (0,\pi)\backslash\{\pi/2\}$	(2.25)	(2.35)

Once we determine the constants C_j for p in a particular case, we will refer to our function p by P_k where k is the case number as outlined in Table 1. We begin with our first critical point (y_1, p_1).

Case 1: Let $\alpha = 0$. It is immediately apparent upon examining (1.2) that $C_1 = 0$. After algebraic manipulation where we substitute in the formulas for y, p given by (2.10) and (2.13), respectively, and isolate for C_3, boundary condition (1.9) gives us

$$C_3 = \frac{1}{2\sqrt{\lambda_1 r(0)}}\Big[\psi\sinh(2\sqrt{\lambda_1}g(1)) - \int_0^1 q(s)\sinh(2\sqrt{\lambda_1}g(s))ds\Big].$$

Hence, the predesign for an arbitrary (continuous) q is given by

$$P_1(x) = \frac{\psi\sinh(2\sqrt{\lambda_1}g(1)) - \int_x^1 q(s)\sinh(2\sqrt{\lambda_1}g(s))ds}{2\sqrt{\lambda_1 r(x)}\cosh^2(\sqrt{\lambda_1}g(x))}. \tag{2.19}$$

Case 2: Let $\alpha = \pi/2$. Boundary condition (1.8) gives us

$$C_3\sqrt{\frac{r(0)}{k}}\cosh(C_1) = 0.$$

We begin by assuming $\cosh(C_1) = 0$, which implies that $C_{1,n} = \frac{2n-1}{2}\pi i$ where $n \in \mathbb{Z}$. If we examine this $C_{1,n}$ in context of our p_1 we find that

$$\begin{aligned}
p_1(x) &= \frac{\int_0^x q(s)\sinh(2\sqrt{\lambda_1}g(s) + (2n-1)\pi i)ds}{2\sqrt{\lambda_1 r(x)}\cosh^2(\sqrt{\lambda_1}g(x) + (n-1/2)\pi i)} \\
&= -\frac{\int_0^x q(s)\sinh(2\sqrt{\lambda_1}g(s))ds}{2\sqrt{\lambda_1 r(x)}(i^2)\sinh^2(\sqrt{\lambda_1}g(x))} \\
&= \frac{\int_0^x q(s)\sinh(2\sqrt{\lambda_1}g(s))ds}{2\sqrt{\lambda_1 r(x)}\sinh^2(\sqrt{\lambda_1}g(x))}.
\end{aligned}$$

If alternately, we assume that $C_3 = 0$, then

$$p_1(x) = \frac{\int_0^x q(s)\sinh(2\sqrt{\lambda_1}g(s) + 2C_1)ds}{2\sqrt{\lambda_1 r(x)}\cosh^2(\sqrt{\lambda_1}g(x) + C_1)},$$

which attains zero at $x = 0$. This can be circumvented if $\cosh(C_1) = 0$. In any event, we conclude that our predesign P_2 takes the form

$$P_2(x) = \frac{\int_0^x q(s)\sinh(2\sqrt{\lambda_1}g(s))ds}{2\sqrt{\lambda_1 r(x)}\sinh^2(\sqrt{\lambda_1}g(x))}. \tag{2.20}$$

Case 3: Let $\alpha \notin \{0, \pi/2\}$. Boundary condition (1.8) implies that

$$C_3 = -\frac{1}{\sqrt{\lambda_1 r(0)}}\phi\tanh(C_1). \tag{2.21}$$

Consider boundary condition (1.9) formulated as in (2.16) and substitute the pair of critical functions $\{y_1, p_1\}$, then

$$\psi = \frac{\int_0^1 q(s)\sinh(2\sqrt{\lambda_1}g(s) + 2C_1)ds}{\sinh(2\sqrt{\lambda_1}g(1) + 2C_1))} + C_3\frac{2\sqrt{\lambda_1 r(0)}\cosh^2(C_1)}{\sinh(2\sqrt{\lambda_1}g(1) + 2C_1))}. \tag{2.22}$$

Here we have essentially a system of two equations with two unknowns: our constant terms C_1 and C_3. If we isolate the term C_3 in (2.22), then we may equate (2.21) and (2.22) to eliminate the term C_3 entirely and arrive at an equality which we may solve for C_1. Indeed, Trigonometry shows that the next equation is a linear algebraic equation for $\tanh(C_1)$.

$$\begin{aligned}
-\phi\tanh(C_1) = \frac{1}{2\cosh^2(C_1)}\Big[&\psi\sinh(2\sqrt{\lambda_1}g(1) + 2C_1) \\
&- \int_0^1 q(s)\sinh(2\sqrt{\lambda_1}g(s) + 2C_1)ds\Big] \quad \Longrightarrow C_1 = z.
\end{aligned} \tag{2.23}$$

Here z is as defined in (2.18). This in turn means for C_3 that

$$C_3 = -\frac{1}{\sqrt{\lambda_1 r(0)}}\phi\tanh(z). \tag{2.24}$$

Then for predesign P_3 we have

$$\begin{aligned} P_3(x) = &\frac{\int_0^x q(s)\sinh(2\sqrt{\lambda_1}g(s)+2z)ds}{2\sqrt{\lambda_1 r(x)}\cosh^2(\sqrt{\lambda_1}g(x)+z)} \\ &- \frac{\phi\sinh(2z)}{2\sqrt{\lambda_1 r(x)}\cosh^2(\sqrt{\lambda_1}g(x)+z)}. \end{aligned} \tag{2.25}$$

We now consider our second critical point (y_2, p_2).

Case 4: Let $\alpha = 0$. Then condition (1.8) implies that

$$\frac{1}{\sqrt{\lambda_1 k}}\cosh(C_2) = 0.$$

We begin with the assumption that $\cosh(C_2) = 0$, which implies that $C_{2,n} = \frac{2n-1}{2}\pi i$ where $n \in \mathbb{Z}$. If we examine this $C_{2,n}$ in context of $p_2(x)$ we find that

$$p_2(x) = \frac{\int_0^x q(s)\sinh(2\sqrt{\lambda_1}g(s))ds}{2\sqrt{\lambda_1 r(x)}\cosh^2(\sqrt{\lambda_1}g(x))} + C_4\frac{\sqrt{r(0)}}{\sqrt{r(x)}\cosh^2(\sqrt{\lambda_1}g(x))}.$$

Condition (1.9) gives us

$$\psi = \frac{\int_0^1 q(s)\sinh(2\sqrt{\lambda_1}g(s))ds}{\sinh(2\sqrt{\lambda_1}g(1))} + C_4\frac{\sqrt{\lambda_1 r(0)}}{\sinh(2\sqrt{\lambda_1}g(1))}$$

which implies

$$C_4 = \frac{1}{2\sqrt{\lambda_1 r(0)}}\Big[\psi\sinh(2\sqrt{\lambda_1}g(1)) - \int_0^1 q(s)\sinh(2\sqrt{\lambda_1}g(s))ds\Big].$$

Thus we find the predesign

$$\begin{aligned} P_4(x) = &\frac{1}{2\sqrt{\lambda_1 r(x)}\cosh^2(\sqrt{\lambda_1}g(x))}[\psi\sinh(2\sqrt{\lambda_1}g(1)) \\ &- \int_x^1 q(s)\sinh(2\sqrt{\lambda_1}g(s))ds] = P_1(x). \end{aligned}$$

Since $P_4(x) \equiv P_1(x)$, our two points of optimality resolve into one critical point, and we refer instead to P_1 only at $\alpha = 0$ (see Table 1).

Case 5: Let $\alpha = \frac{\pi}{2}$. Condition (1.8) implies

$$C_4\sqrt{\frac{r(0)}{k}}\sinh(C_2) = 0.$$

In the case $C_{2,n} = \pi i n$, where $n \in \mathbb{Z}$, p_2 becomes

$$p_2 = \frac{\int_0^x q(s)\sinh(2\sqrt{\lambda_1}g(s))ds}{2\sqrt{\lambda_1 r(x)}\sinh^2(\sqrt{\lambda_1}g(x))}.$$

In the case $C_4 = 0$, we see that

$$p_2 = \frac{\int_0^x q(s)\sinh(2\sqrt{\lambda_1}g(s)+2C_2)ds}{2\sqrt{\lambda_1 r(x)}\sinh^2(\sqrt{\lambda_1}g(x)+C_2)}.$$

This function is zero at $x = 0$, and therefore, unsuitable as a design unless we require that $C_2 = 0$. Since $P_5(x) \equiv P_2(x)$, similar to the immediately preceding case we note that the two points of optimality resolve themselves into one and we refer to P_2 only at $\alpha = \pi/2$ (see Table 1).

Case 6: Let $\alpha \notin \{0, \pi/2\}$. Isolation of the term C_4 in (1.8) yields

$$C_4 = -\frac{1}{\sqrt{\lambda_1 r(0)}} \phi \coth(C_2). \tag{2.26}$$

If we consider boundary condition (1.9) formulated as in (2.16) and substitute the pair of critical functions $\{y_2, p_2\}$, then

$$\psi = \frac{\int_0^1 q(s) \sinh(2\sqrt{\lambda_1} g(s) + 2C_2) ds}{\sinh(2\sqrt{\lambda_1} g(1) + 2C_2))} + C_4 \frac{2\sqrt{\lambda_1 r(0)} \sinh^2(C_2)}{\sinh(2\sqrt{\lambda_1} g(1) + 2C_2))}. \tag{2.27}$$

After algebraic manipulations, we may combine (2.26) and (2.27) to solve for C_2. We find

$$\begin{aligned} -\phi \coth(C_2) = \frac{1}{2\sinh^2(C_2)} \Big[&\psi \sinh(2\sqrt{\lambda_1} g(1) + 2C_2) \\ &- \int_0^1 q(s) \sinh(2\sqrt{\lambda_1} g(s) + 2C_2) ds \Big], \end{aligned}$$

which implies

$$C_2 = z. \tag{2.28}$$

Here z is as defined in (2.18). This in turn means for C_4 that

$$C_4 = -\frac{1}{\sqrt{\lambda_1 r(0)}} \phi \coth(z). \tag{2.29}$$

Therefore, we have a predesign at $\alpha \notin \{0, \frac{\pi}{2}\}$ given by

$$\begin{aligned} P_6(x) = &\frac{\int_0^x q(s) \sinh(2\sqrt{\lambda_1} g(s) + 2z) ds}{2\sqrt{\lambda_1 r(x)} \sinh^2(\sqrt{\lambda_1} g(x) + z)} \\ &- \frac{\phi \sinh(2z)}{2\sqrt{\lambda_1 r(x)} \sinh^2(\sqrt{\lambda_1} g(x) + z)}. \end{aligned} \tag{2.30}$$

However, we now have two critical points at this α. Since the numerators in P_3 and P_6 are identical, we only need to compare the denominators of the two P_3 and P_6, which are always positive. Thus there is no place where P_6 could be positive and P_3 negative. If we examine the ratio of P_3 and P_6, we see that

$$\frac{P_3}{P_6} = \frac{\sinh^2(\sqrt{\lambda_1} g(x) + z)}{\cosh^2(\sqrt{\lambda_1} g(x) + z)} < 1.$$

We conclude that the mass generated by P_3 will be inferior to the mass generated by P_6 - and thus P_6 is a superfluous solution. Of our two points of optimality, we will refer only to P_3 at $\alpha \notin \{0, \pi/2\}$.

2.3. **Determining attendant solvability conditions and optimal masses.** This subsection is devoted to the derivation of conditions on the given data set $\mathscr{D}$ such that a positive design p exists as well as to the determination of the mass $M[p]$ if these conditions are met.

Case 1: Let P_1 be as in (2.19). The denominator, $2\sqrt{\lambda_1 r(x)} \cosh^2(\sqrt{\lambda_1} g(x))$, is positive everywhere on the domain, so we focus solely on the numerator to determine the sign. We find that

$$\psi \sinh(2\sqrt{\lambda_1} g(1)) - \int_x^1 q(s) \sinh(2\sqrt{\lambda_1} g(s)) ds > 0$$

which implies

$$\int_x^1 q(s)\sinh(2\sqrt{\lambda_1}g(s))ds < \psi\sinh(2\sqrt{\lambda_1}g(1)), \quad \forall x \in [0,1]. \tag{2.31}$$

Also, at the boundary $x = 1$, our term containing the integral vanishes. Thus to guarantee the positivity of the design, we have to require

$$\psi > 0. \tag{2.32}$$

If both of these conditions are met, we refer to our P_1 as a design rather than a predesign, and we have the optimal mass

$$\begin{aligned} M[P_1] &= \int_0^1 r(x)\frac{1}{2\sqrt{\lambda_1 r(x)}\cosh^2(\sqrt{\lambda_1}g(x))}\Big[\psi\sinh(2\sqrt{\lambda_1}g(1)) \\ &\quad - \int_x^1 q(s)\sinh(2\sqrt{\lambda_1}g(s))ds\Big]\,dx \\ &= \frac{1}{\lambda_1}\Big[\psi\sinh^2(\sqrt{\lambda_1}g(1)) - \int_0^1 q(s)\sinh^2(\sqrt{\lambda_1}g(s))ds\Big]. \end{aligned} \tag{2.33}$$

Case 2: Let P_2 be as in (2.20). Here we have a potential discontinuity at $x = 0$. We proceed via L'Hopital's Rule.

$$\lim_{x\to 0} p_2 = \lim_{x\to 0}\frac{\int_0^x q(s)\sinh(2\sqrt{\lambda_1}g(s))ds}{2\sqrt{\lambda_1 r(x)}\sinh^2(\sqrt{\lambda_1}g(x))} = \frac{q(0)}{2\lambda_1 r(0)}.$$

Thus we have a positive design that is continuous at $x = 0$ if $q(x) > 0$ along $[0,1]$. If this condition is met we have a mass given by

$$\begin{aligned} M[P_2] &= \int_0^1 r(x)\frac{\int_0^x q(s)\sinh(2\sqrt{\lambda_1}g(s))ds}{2\sqrt{\lambda_1 r(x)}\sinh^2(\sqrt{\lambda_1}g(x))}dx \\ &= \frac{1}{2\lambda_1}\Big[2\int_0^1 q(s)\cosh^2(\sqrt{\lambda_1}g(s))ds \\ &\quad - \coth(\sqrt{\lambda_1}g(1))\int_0^1 q(s)\sinh(2\sqrt{\lambda_1}g(s))ds\Big]. \end{aligned} \tag{2.34}$$

Case 3: Let P_3 be as in (2.25). The denominator is positive everywhere in the domain, so we may focus on the numerator. We formulate the condition

$$\int_0^x q(s)\sinh(2\sqrt{\lambda_1}g(s) + \coth^{-1}(\zeta))ds - \phi\sinh(\coth^{-1}(\zeta)) > 0, \quad \forall x \in [0,1].$$

At $x = 0$, this implies $\phi\sinh(\coth^{-1}(\zeta)) < 0$. For $\alpha \in (0, \frac{\pi}{2})$, $\phi > 0$ so we must require

$$\sinh(\coth^{-1}(\zeta)) < 0 \implies \zeta < -1$$

The above inequalities imply $\zeta > 1$ for $\alpha \in (\frac{\pi}{2}, \pi)$. If these conditions are met, we refer to P_3 as a design and we have mass

$$\begin{aligned} M[P_3] &= \int_0^1 r(x)\Big[\frac{\int_0^x q(s)\sinh(2\sqrt{\lambda_1}g(s)+\coth^{-1}(\zeta))ds}{2\sqrt{\lambda_1 r(x)}\cosh^2(\sqrt{\lambda_1}g(x)+\frac{1}{2}\coth^{-1}(\zeta))} \\ &\quad - \frac{\phi\sinh(\coth^{-1}(\zeta))}{2\sqrt{\lambda_1 r(x)}\cosh^2(\sqrt{\lambda_1}g(x)+\frac{1}{2}\coth^{-1}(\zeta))}\Big]dx \\ &= \frac{1}{2\lambda_1}\Big[\tanh(\sqrt{\lambda_1}g(1)+z)(\int_0^1 q(x)\sinh(2\sqrt{\lambda_1}g(x)+2z)dx \\ &\quad - \phi\sinh(2z)) - 2(\int_0^1 q(x)\sinh^2(\sqrt{\lambda_1}g(x)+z)dx - \phi\sinh^2(z))\Big]. \end{aligned} \tag{2.35}$$

Now that we have our solvability conditions on our data sets $\mathscr{D}$, we devote the next section to an exploration of the character of our sets $\mathscr{P}$ and $\mathscr{P}^c$ as well as Remark 1.7.

3. Numerical examples and exceptional cases

3.1. **Characteristics of sets $\mathscr{P}$ and $\mathscr{P}^c$.** By way of illustration, we introduce the following pair of numerical examples using the data set

$$\mathscr{D} = \{q(x) = -x^2, r(x) = 1, \alpha = 0, \beta_1 = \beta_2' = 0, \beta_1' = \beta_2 = 1, \lambda_1 = 2\}.$$

Here we introduce a nonzero q to Turner's [20] work and return a design and mass. Retaining the same data set, we vary ψ slightly to illustrate how we may radically alter p and $M[p]$ by breaking our solvability conditions (2.31) and (2.32). We include two complementary illustrations (Figures 1 and 2). In both figures, we multiply the ψ given in the data set by a small scalar c. To generate these figures, we use the algorithm in the form of a Python script detailed in [23]. This script takes the array $\mathscr{D}$, uses the data to determine the case according to Table 1, generates the constants ϕ, ψ, and then checks the relevant solvability conditions.

- In Figure 1, we take small variations of positive ψ with $c \in [0.5, 1.5]$, while not breaking the solvability conditions on our $p(x)$. We consequently observe very little deformation of the curve $p(x)$ and a narrow range of variance in our calculated masses $M[P_1]$. In other words, the distance between the mass generated by the topmost function p and bottommost p graphed in Figure 1 is relatively narrow.
- However, in Figure 2, we vary between $c \in [-1, 1]$. The negative $c\psi$ does violate our solvability conditions and, consequently, shows a dramatic deformation of the graph as well as a much wider spread in our range of variance in calculated masses - here the distance between the mass generated by the topmost p and bottommost p graphed in Figure 2 is much broader than in Figure 1. For the purpose of comparison, we have calculated all of the masses implied by the data sets used in Figure 2 even if they fail our solvability conditions and return negative values for $M[p]$.

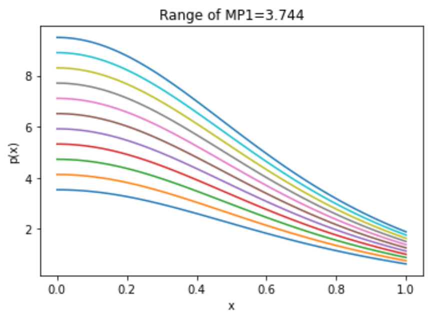

FIGURE 1. Illus. 1

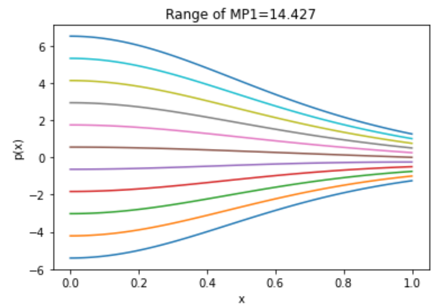

FIGURE 2. Illus. 2

We return to Remark 1.7 for a brief explanation of the closeness of our two sets $\mathscr{P}, \mathscr{P}^c$ as it pertains specifically to $P_1(x)$. Say that we have two data sets $\mathscr{D}_1$ and $\mathscr{D}_2$ which are identical except for the terms ψ and q. We let $0 < |\psi_j| << 1,\ j = 1, 2$ but ψ_1 positive and ψ_2 negative; while we define q_1 and q_2 as

$$q_1 = 2\psi_1\sqrt{\lambda_1 r}, \quad q_2 = 2\psi_2\sqrt{\lambda_1 r}.$$

Note that while both data sets satisfy (2.31), $\mathscr{D}_2$ fails to satisfy (2.32). We observe that $\|q_1 - q_2\|_{C[0,1]} \leq 2\sqrt{\lambda_1}\max_{[0,1]}\sqrt{r}|\psi_1 - \psi_2|$, which is small enough if $|\psi_1 - \psi_2|$ is small enough. This explicitly demonstrates that while the sets $\mathscr{P}$ and $\mathscr{P}^c$ do not overlap, they do contain elements p whose generating data sets are arbitrarily close.

3.2. **General Numerical Examples.** To further illustrate the nature of our critical functions $p(x)$, we present several numerical examples of potential designs that do (do not) meet the solvability conditions we have described. The Python script used to algorithmically generate these figures is detailed in [23].

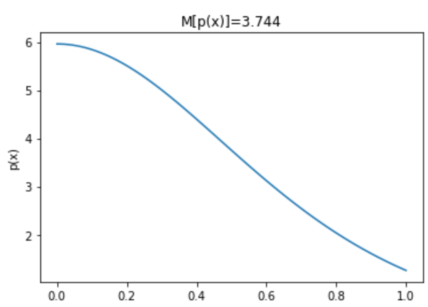

FIGURE 3. Example 1

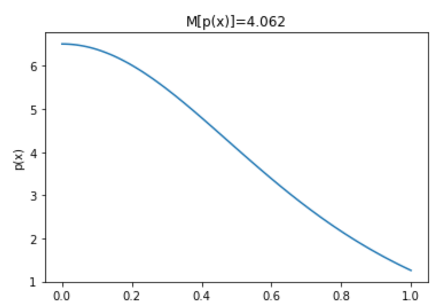

FIGURE 4. Example 2

(1) $\mathscr{D} := \{q = 0, r = 1, \alpha = 0, \beta_1 = 0, \beta_1' = 1, \beta_2 = 1, \beta_2' = 0, \lambda_1 = \lambda\}$. This was the system that Turner studied in [20] where λ is left as an arbitrary positive constant. It may be shown that our formula (2.19) for p and (2.33) for mass return the same results. Namely, for our critical $p(x)$ and mass $M[p]$ we find

$$p(x) = \frac{\sqrt{\lambda_1}\sinh(2\sqrt{\lambda_1})}{2\cosh^2(\sqrt{\lambda_1}x)}, \quad M[p(x)] = \sqrt{\lambda_1}\sinh^2(\sqrt{\lambda_1}).$$

If we go further and assign a numerical value to λ_1, say $\lambda_1 = 2$, we can present a numerical value for $M[p]$ and the graph of $p(x)$ (Figure 3).

(2) $\mathscr{D} := \{q = -x^2, r = 1, \alpha = 0, \beta_1 = 0, \beta_1' = 1, \beta_2 = 1, \beta_2' = 0, \lambda_1 = 2\}$. Here we introduce a nonzero $q(x)$ to Turner's work and return a design and mass (Figure 4).

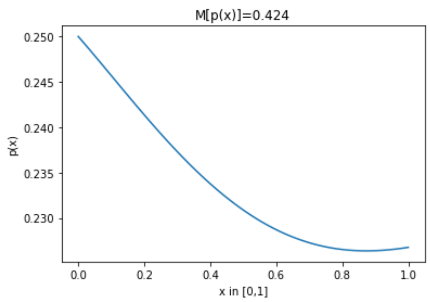

FIGURE 5. Example 3

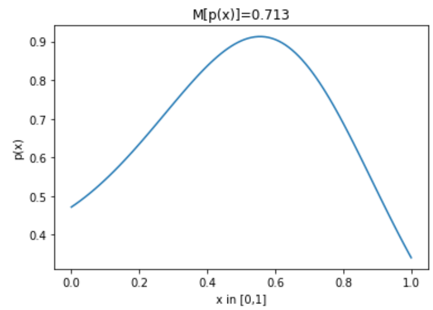

FIGURE 6. Example 4

(3) $\mathscr{D} := \{q = r = x^2 + x + 1, \alpha = \frac{\pi}{2}, \beta_1 = 1, \beta_1' = 5, \beta_2 = 1, \beta_2' = 2, \lambda_1 = 2\}$. Notably, this example would not return a nonzero result under the earlier assumption (see [7]) that $q \equiv 0$. Here, however, we meet the solvability condition and return a positive mass (Figure 5).

(4) $\mathscr{D} := \{q = -x, r = 1 + 2x, \alpha = \frac{\pi}{4}, \beta_1 = 1, \beta_1' = 10, \beta_2 = 5, \beta_2' = 10, \lambda_1 = 2\}$. At $\alpha \notin \{0, \frac{\pi}{2}\}$, our optimal p is P_3. This data set meets our solvability conditions, and our algorithm returns a positive mass (Figure 6). We note that, unlike the optimal designs in Figure 3 and Figure 4, the designs in Figure 5 and Figure 6) are not monotonic.

3.3. **Exceptional cases for λ_1 and ψ.** As we mentioned in Remark 1.4, the number of negative eigenvalues λ_1 is at most finite, and we assume $\lambda_1 > 0$ everywhere above. We now briefly discuss the opposite case, $\lambda_1 \leq 0$. We omit technicalities here and only show the results. The full details may be found in [18].

For $\lambda_1 < 0$, the predesigns have the form

$$P_1 = \frac{\psi \sin(2\sqrt{|\lambda_1|}g(1)) - \int_x^1 q(s)\sin(2\sqrt{|\lambda_1|}g(s))ds}{2\sqrt{|\lambda_1| r(x)}\cos^2(\sqrt{|\lambda_1|}g(x))}, \tag{3.1}$$

$$P_2 = -\frac{\int_0^x q(s)\sin(2\sqrt{|\lambda_1|}g(s))ds}{2\sqrt{|\lambda_1| r(x)}\sin^2(\sqrt{|\lambda_1|}g(x))}, \tag{3.2}$$

$$P_3 = \frac{\int_0^x q(s)\sin(2\sqrt{|\lambda_1|}g(s) + z')ds - \phi\sin(2z')}{2\sqrt{|\lambda_1| r(x)}\cos^2(\sqrt{|\lambda_1|}g(x) + z')}, \tag{3.3}$$

with corresponding masses given by

$$M[P_1] = \frac{1}{|\lambda_1|}\Big[\psi\sin^2(\sqrt{|\lambda_1|}g(1)) - \int_0^1 q(s)\sin^2(\sqrt{|\lambda_1|}g(s))ds\Big], \tag{3.4}$$

$$M[P_2] = \frac{1}{2|\lambda_1|}\Big[\cot(\sqrt{|\lambda_1|}g(1))\int_0^1 q(x)\sin(2\sqrt{|\lambda_1|}g(x))dx$$

$$- \int_0^1 q(x) \sin(2\sqrt{|\lambda_1|}g(x)) \cot(\sqrt{|\lambda_1|}g(x))dx\Big], \tag{3.5}$$

$$\begin{aligned} M[P_3] = \frac{1}{2|\lambda_1|}\Big[\tan(\sqrt{|\lambda_1|}g(1) + z')\Big(\int_0^1 q(x) \sin(2\sqrt{|\lambda_1|}g(x) + 2z')dx \\ - \phi \sin(2z')\Big) - 2\Big(\int_0^1 q(x) \sin^2(\sqrt{|\lambda_1|}g(x) + z')dx - \phi \sin^2(z')\Big)\Big], \end{aligned} \tag{3.6}$$

subject to solvability conditions which we omit here.

For $\lambda_1 = 0$, interestingly, we do not show the same behavior, i.e., we do not observe predesigns for all cases. We find that only

$$\lim_{\lambda_1 \to 0} P_1(x) = \frac{1}{\sqrt{r(x)}}[\psi g(1) - \int_x^1 q(s)g(s)ds], \tag{3.7}$$

is defined and has mass

$$M[P_1] = \psi g^2(1) - \int_0^1 q(x)g^2(x)dx, \tag{3.8}$$

subject to solvability conditions, while the other two predesigns - P_2 and P_3 - do not return any valid designs. We also investigate other exceptional cases in regards to the boundary conditions such as $\psi \to \infty$ or $\psi \to 0$ in the limiting sense. We summarize them only briefly. The full, rigorous discussion of these predesigns may be found in [18]. To begin, we consider the case where $\psi \to \infty$. If we take P_1 (2.19), then clearly

$$\lim_{\psi \to \pm\infty} P_1 = \infty \implies P_1 \notin \mathscr{P}.$$

That is to say, we have no hope of returning a design for P_1 under these conditions. While ψ is not present in P_2, we observe that ψ is a component of ζ (2.17) and will therefore have an effect on P_3. We conclude that as $\psi \to \infty$,

$$\lim_{\psi \to \infty} P_3 = \frac{- \int_0^x q(s) \sinh(2\sqrt{\lambda_1}(g(1) - g(s)))ds + \phi \sinh(2\sqrt{\lambda_1}g(1))}{2\sqrt{\lambda_1 r(x)} \cosh^2(\sqrt{\lambda_1}(g(1) - g(x)))}.$$

Subject to solvability conditions, both $p \in \mathscr{P}$ and $p \notin \mathscr{P}$ are possible. We also consider the case that $\psi \to 0$. For P_1 we observe that

$$\psi = 0 \implies P_1(x) = -\frac{1}{2\sqrt{\lambda_1 r(x)} \cosh^2(\sqrt{\lambda_1}g(x))} \int_x^1 q(s) \sinh(2\sqrt{\lambda_1}g(s))ds.$$

Here we see that at $x = 1$, $P_1(x) = 0$. We conclude that there is no design under these conditions. In regards to P_3, observe that at $\psi = 0$, from (2.17) and (2.18), while the exact value of these constants will be changed, the overall character of predesign P_3 will remain unchanged. Therefore we may still have both $p(x) \in \mathscr{P}$ and $p(x) \notin \mathscr{P}$.

3.4. **Schematic of solvability conditions.** What follows is a representation of our solvability conditions applied to a given data set. While our solvability conditions and code may produce results for a more general data set, in this particular example the data set $\mathscr{D}$ is of the type that would produce Case 1.

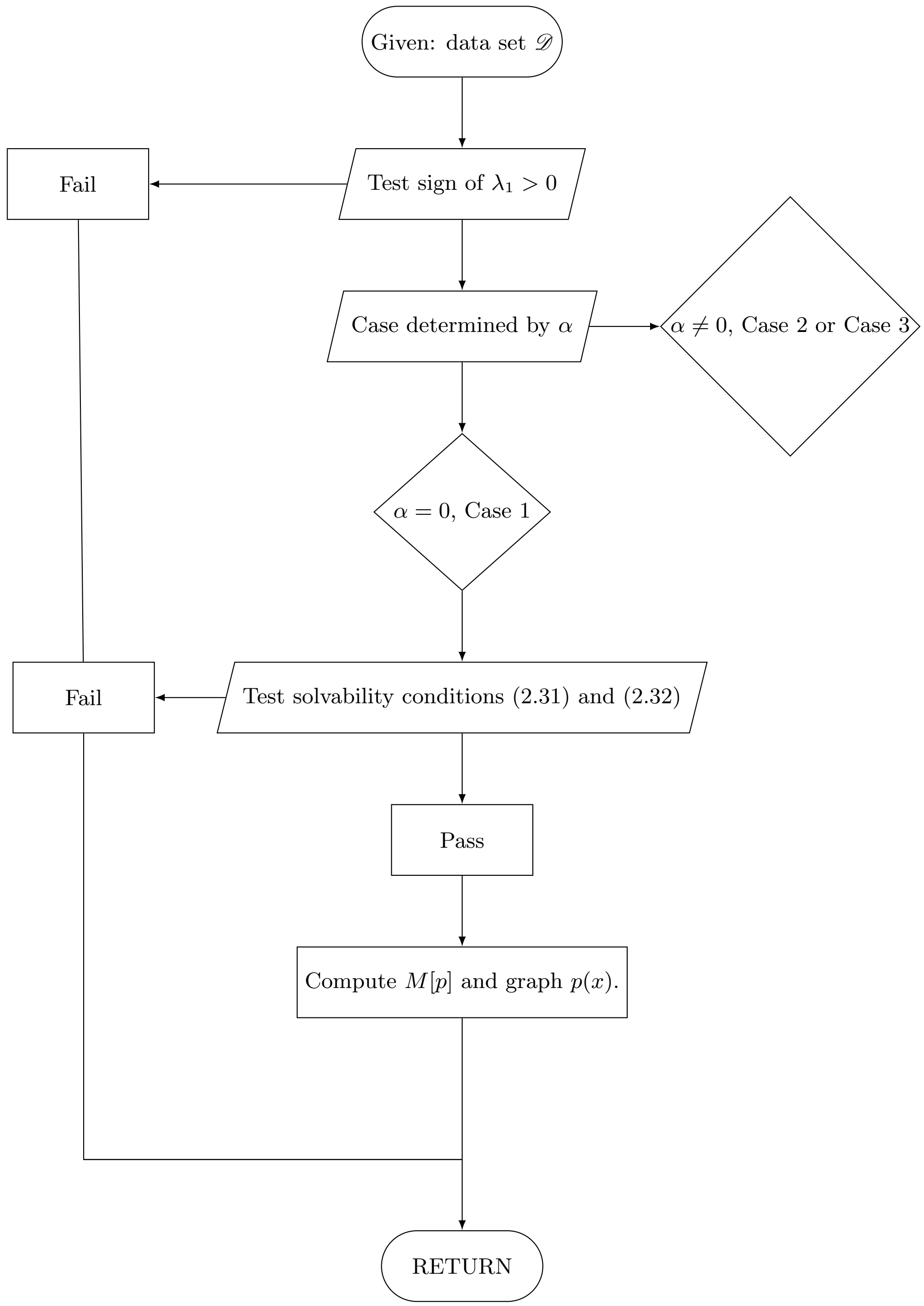
Given: data set $\mathscr{D}$
Fail
Test sign of $\lambda_1 > 0$
Case determined by α
$\alpha \neq 0$, Case 2 or Case 3
$\alpha = 0$, Case 1
Fail
Test solvability conditions (2.31) and (2.32)
Pass
Compute $M[p]$ and graph $p(x)$.
RETURN

FIGURE 7.

4. Conclusion and discussion

We consider the optimal design problem modeled by a linear second-order, regular Sturm-Liouville problem on a finite interval with the spectral parameter in one of the boundary conditions. We find the explicit formulas for the potential optimal design. We analyze the intervals of the parameters of the problem where such a design exists. A similar problem for a particular case of the Sturm-Liouville operator was previously considered by one of the authors, however, we bypass the results of that paper in four aspects. (a) In that publication, it was claimed that the optimization problem for the general linear Sturm-Liouville operator of the second order may not be treated analytically and only numerical optimization is a hope. Here, we find the optimal design $\forall q \not\equiv 0$ explicitly. (b) Further, only the critical points of the functional were found. We now call them the predesigns. It was not analyzed whether the predesigns produced the actual, physically meaningful, designs. This analysis is performed here and results in the solvability conditions that have the form of the restrictions of the data set. (c) The physical meaning of the spectral parameter (for the known mechanical problems) is the eigenfrequency. Hence, for the mechanical problems, we must assume that the parameter is positive. Yet, for mathematical completeness, we mention optimization results for non-positive values of the spectral parameter (which the Spectral Theory allows). (d) We create a code that allows finding a design - if it exists - for any given data.

As a result of generalizations (a) and (c), we find that the set of designs is broader than in the known papers [20] and [19], as well as the previous author's paper [7]. Initially, we found two critical points for all cases of α. However, these were resolved to prove that there is indeed a unique critical point - and thus predesign - for all α. Further, we show that a unique design - not only predesign - exists $\forall \mathscr{D}$ which passes our solvability conditions. The results (a) – (c) above represent the main pleasant moments of this study. We also mention the existence of a solution corresponding to the design $p_2(x)$, not only to $p_1(x)$, though this was observed in the previous author's paper [7] for the particular case $q \equiv 0$.

Based on the duality that was derived in [19] for the mechanical version of our problem, we may expect that the following two problems have the same optimal solution $p(x)$:

1. Given the data set $\mathscr{D}_1 = \{\alpha, \beta_1, \beta_2, \beta_1', \beta_2', \lambda_1, q, r\}$, find $p(x)$ such that $M[p] \to$ min.
2. Given the data set $\mathscr{D}_2 = \{\alpha, \beta_1, \beta_2, \beta_1', \beta_2', q, r, M\}$, find $p(x)$ such that $\lambda_1[p] \to$ max.

We have contributed to Problem 1.1 but may hope that the optimal p from solving Problem 1.1 is the same as the optimal p from solving Problem 1.3. The validity of this duality in the case of multiple critical points and solvability conditions (restrictions on the data set) should be studied further especially because, for an arbitrary variational problem, the duality may not hold (see [15]).

Acknowledgments. B. P. Belinskiy was partially supported by the Tennessee Higher Education Commission through the Center of Excellence in Applied Computational Science and Engineering (CEACSE) at the University of Tennessee at Chattanooga grant. T. A. Smith would like to thank the Department of Mathematics at the University of Alabama at Birmingham for supporting this research. The authors are grateful to the anonymous referees for their various recommendations for the improvement of this manuscript.

References

[1] W. O. Amrein, A. M. Hinz, D. P. Pearson; Sturm-Liouville Theory: Past and Present, *Birkhauser Basel*, Basel, Switzerland, 2005.

[2] S. A. Avdonin, B. P. Belinskiy; On controllability of a rotating string, *J. of Math. Analysis and Applications*, 321 (1) (2006), 198-212.

[3] B. P. Belinskiy, J. P. Dauer; On a regular Sturm-Liouville problem on a finite interval with the eigenvalue parameter appearing linearly in the boundary conditions, *Spectral Theory and Computational Methods of Sturm-Liouville Problems*, ed. by D. Hinton and P. W. Schaefer, Marcel Dekker, Inc. New York (1997), 183-196.

[4] B. P. Belinskiy, J. P. Dauer; Eigenoscillations of mechanical systems with boundary conditions containing the frequency, *Quarterly Appl. Math*, 56 (3) (1998), 521-541.

[5] B. P. Belinskiy, J. W. Hiestand, L. Weerasena; Optimal design of a fin in steady-state, *Appl. Mathem. Model.*, 77, Part 2 (2020), 1188-1200.

[6] B. P. Belinskiy, D. B. Hinton, L. Weerasena, M. Khan; On the Sturm-Liouville problem describing an ocean waveguide covered by pack ice, *Applicable Analysis*, 101 (5) (2021), 1659-1681.

[7] B. P. Belinskiy, D. H. Kotval; Optimal design of minimum mass structures for a generalized Sturm-Liouville problem on an interval and a metric graph, *Electron. J. Diff. Equ.*, 119 (2018), 1-18.

[8] B. P. Belinskiy, J. V. Matthews, J. W. Hiestand; Piecewise uniform optimal design of a bar with an attached mass, *Electron. J. Diff. Equ.*, 133 (2015), 1-17.

[9] C. T. Fulton; Two-point boundary value problems with eigenvalue parameter contained in the boundary conditions, *Proc. Roy. Soc. Edinburg*, 77A (1977), 293-308.

[10] C. T. Fulton; Singular eigenvalue problems with eigenvalue parameter contained in the boundary conditions, *Proc. Roy. Soc. Edinburg*, 87A (1980), 1-34.

[11] I. M. Gelfand, S. V. Fomin; Calculus of Variations, *Dover*, Mineola, New York, 1963.

[12] D. Hinton; An expansion theorem for an eigenvalue problem with eigenvalue parameter in the boundary condition, *Quart. J. Math.*, 30 (1979), 33-42.

[13] D. Hinton, M. McCarthy; Bounds and optimization of the minimum eigenvalue for a vibrating system, *Electron. J. Dif. Equ.*, 48 (2013), 1-22.

[14] K. R. Mamedov, F. A. Cetinkaya; Inverse problem for a class of Sturm-Liouville operator with spectral parameter in boundary condition, *Boundary Value Problems*, 183 (2013), 1-16.

[15] B. Mond and M. A. Hanson; Duality for variational problems, *J of Math Anal. Applic.*, 18 (1967), 355-364.

[16] V. Pivovarchyk; Inverse Sturm-Liouville problem for a star graph by three spectra, *Operators and Matrices*, 12 (2018), 1-18.

[17] Y. Shioji; The spectral properties of boundary–value problems with eigenvalue parameter in the boundary conditions, *MS thesis, The University of Tennessee, Knoxville*, 1995.

[18] T. Smith; Optimization for a Sturm-Liouville Problem with the spectral parameter in the boundary condition, *Ph.D. thesis, The University of Tennessee, Chattanooga*, 2022.

[19] J. E. Taylor; Minimum mass bar for axial vibration at specified natural frequency, *AIAA Journal*, 5 (10) (1967) 1911-1913.

[20] M. J. Turner; Design of minimum mass structures with specified natural frequencies, *AIAA Journal*, 5 (3) (1967), 406-412.

[21] J. Walter; Regular eigenvalue problems with eigenvalue parameter in the boundary condition, *Math. Z.* 133 (1973), 301-312.

[22] A. Zettl; Sturm-Liouville Theory, *Mathematical Surveys and Monographs*, v. 121, Rhode Island: American Mathematical Society, 2005.

[23] T. A. Smith; *optimSL*, [Python] (2022) *https : //github.com/smithtannera/optim*

Boris P. Belinskiy (corresponding author)
University of Tennessee at Chattanooga, Department of Mathematics, Dept 6956, 615 McCallie Ave., Chattanooga, TN 37403-2598, USA
Email address: boris-belinskiy@utc.edu

Tanner A. Smith
University of Alabama at Birmingham, Department of Mathematics, Room 4005, 10th Ave S, Birmingham, AL 35294, USA
Email address: tsmith46@uab.edu